Chinese Journal of Natural Medicines

Paeoniflorin alleviates depression by inhibiting the activation of NLRP3 inflammasome *via* promoting mitochondrial autophagy

Lili SU, Pengli GUO, Xiangjuan GUO, Zhongmei HE, Yan ZHAO, Ying ZONG, Jianming LI, Weijia CHEN, Rui DU

Citation: Lili SU, Pengli GUO, Xiangjuan GUO, Zhongmei HE, Yan ZHAO, Ying ZONG, Jianming LI, Weijia CHEN, Rui DU, Paeoniflorin alleviates depression by inhibiting the activation of NLRP3 inflammasome *via* promoting mitochondrial autophagy, Chinese Journal of Natural Medicines, 2024, 22(6), 515−529. doi: 10.1016/S1875−5364(24)60654−0.

View online: https://doi.org/10.1016/S1875−5364(24)60654−0

Available online at www.sciencedirect.com
ScienceDirect
Chinese Journal of Natural Medicines 2024, **22**(6): 515-529
doi: 10.1016/S1875-5364(24)60654-0
Chinese Journal of Natural Medicines

•Original article•

Paeoniflorin alleviates depression by inhibiting the activation of NLRP3 inflammasome *via* promoting mitochondrial autophagy

SU Lili[1], GUO Pengli[1], GUO Xiangjuan[1], HE Zhongmei[1], ZHAO Yan[1], ZONG Ying[1], LI Jianming[1], CHEN Weijia[1*], DU Rui[1, 2, 3*]

[1] *College of Chinese Medicinal Materials, Jilin Agricultural University, Changchun 130118, China;*
[2] *Jilin Provincial Engineering Research Center for Efficient Breeding and Product Development of Sika Deer, Changchun 130118, China;*
[3] *Key Laboratory of Animal Production and Product Quality and Security, Ministry of Education, Ministry of National Education, Changchun 130118, China*

Available online 20 Jun., 2024

[ABSTRACT] Depression ranks among the most common neuropsychiatric disorders globally. Current studies examining the roles of inflammation and mitochondrial autophagy in the antidepressant efficacy of paeoniflorin (PF) are sparse. This study aimed to elucidate PF's antidepressant mechanism by promoting autophagy and inhibiting NLRP3 inflammasome activation using chronic unpredictable mild stimulation (CUMS)-induced C57BL/6 mouse models *in vivo* and corticosterone (CORT)-induced HT22 cell models *in vitro*. Results demonstrated that PF enhanced the viability of HT22 cells following CORT exposure, restored mitochondrial membrane potential (MMP), reduced reactive oxygen species accumulation, increased LC3 fluorescence intensity, and suppressed inflammatory cytokine secretion and inflammation activation. Additionally, PF ameliorated depressive behaviors induced by CUMS and improved damage in hippocampal neurons. It also reduced the expression of NLRP3, ASC, Caspase-1, IL-1β, and the assembly of the NLRP3 inflammasome. Moreover, PF upregulated the expression of autophagy-related proteins in the hippocampus, facilitating the clearance of damaged mitochondria and enhancing autophagy. The role of autophagy in PF's antidepressant effects was further confirmed through the use of the autophagy inhibitor 3-methyladenine (3-MA), which reduced the efficacy of PF. In conclusion, PF effectively improved depressive behaviors in CUMS-induced mice and reduced NLRP3-mediated inflammation both *in vivo* and *in vitro*, likely *via* the induction of autophagy.

[KEY WORDS] Paeoniflorin; Depression; Autophagy; NLRP3 inflammasome
[CLC Number] R965 **[Document code]** A **[Article ID]** 2095-6975(2024)06-0515-15

Introduction

Depression is a chronic mental and emotional disorder [1]. Its primary clinical symptoms include anhedonia, pessimism, emotional instability, cognitive and motor slowing, and sleep disturbances [2]. Depression has been linked to several diseases, such as diabetes [3], Parkinson's disease [4], and various cancers [5], and it is projected to become a major contributor to the global disease burden by 2030 [6].

Paeoniflorin (PF; $C_{23}H_{28}O_{11}$) is a glycoside monoterpene noted for its hepatoprotective [7], anti-inflammatory [8], antitumor [9], immunomodulatory [10], and anti-Parkinsonian [11] effects, as well as its ability to ameliorate cerebral ischemia [12]. Pharmacological studies have demonstrated that the neuroprotective and antidepressant actions of PF involve the regulation of monoamine neurotransmitters [13], the hypothalamic-pituitary-adrenal (HPA) axis [14], oxidative stress [15], and neuron health [16]. However, research into how PF modulates the interaction between autophagy and inflammation to mitigate depression remains scarce.

Autophagy, including mitochondrial autophagy, is a protective intracellular degradation process intricately linked to inflammation [17]. Upon activation, autophagy isolates defective proteins, damaged organelles, and other cellular components in autophagosomes, which are then transferred to lysosomes for degradation [18]. Autophagosomes can also engulf inflammasome components, such as the apoptosis-associated speck-like protein (ASC), thereby preventing their activation

[Received on] 23-Nov.-2023
[Research funding] This work was supported by the Jilin Science &Technology Development Plan (Nos. 20210204001YY and 20200404090YY); Jilin Province aid Project for Xinjiang Uygur Autonomous Region (No. 0207-202020043).
[*]**Corresponding author]** E-mails: chenweijia_jlau@163.com (CHEN Weijia); durui@jlau.edu.cn (DU Rui)
These authors have no conflict of interest to declare.

and reducing inflammation. Additionally, several studies have reported dysregulated autophagy in animal models of depression [19].

The NLRP3 inflammasome is composed of NLRP3, ASC, and Caspase-1. Activation of the NLRP3 inflammasome triggers the cleavage of Caspase-1 and Interleukin-1β (IL-1β), initiating an inflammatory response [20]. Recent studies have demonstrated significant increases in inflammatory reactions within the brains of depressed animals, with an observed overexpression of the NLRP3 inflammasome components in such cases [21, 22].

Interestingly, inhibition of autophagy often results in the substantial accumulation of damaged mitochondria, which promotes the production of mitochondrial reactive oxygen species (ROS) and subsequent activation of the NLRP3 inflammasome [23]. Therefore, autophagy represents a promising therapeutic target for diseases mediated by the NLRP3 inflammasome. Studies have shown that increases in LC3 protein levels, reductions in p62 protein levels, and enhanced autophagy activity can inhibit the activation of NLRP3 inflammasome complexes, which decreases the expressions of NLRP3, ASC, Caspase-1, and IL-1β, thereby alleviating depression-like behaviors [24, 25]. Thus, promoting autophagy can suppress the activation of the NLRP3 inflammasome, improving inflammatory responses in neurological disorders such as depression, Alzheimer's disease, and Parkinson's syndrome [26].

In this context, the current study utilized CUMS-induced mouse models and CORT-induced HT22 cell models to investigate the antidepressant effects of PF through the modulation of mitochondrial autophagy and its interaction with the NLRP3 inflammasome.

Materials and Methods

Materials

Paeoniflorin (PF), fluoxetine hydrochloride (FLU), and corticosterone (CORT) were sourced from Yuanye (Shanghai, China). The autophagy inhibitor 3-methyladenine (3-MA) was obtained from MCE (China). DMEM medium and fetal bovine serum (FBS) were purchased from Gibco (Australia). The Mitochondrial Membrane Potential Assay Kit with JC-1 (JC-1) was supplied by Solarbio (China). The reagents 2, 7-dichlorofluorescein diacetate (DCFH-DA) and the BCA kit, along with the Caspase-1 kit, were provided by Beyotime (China). Enzyme-linked immunosorbent assay (ELISA) kits for IL-1β, IL-18, IL-6, and brain-derived neurotrophic factor (BDNF) were acquired from Enzyme Immunoassay (Jiangsu, China). Additional ELISA kits for serotonin (5-HT) and CORT were purchased from Fantejin (China). Polyvinylidene difluoride (PVDF) membranes were obtained from Merck Millipore (Germany). Antibodies used in this study included anti-LC3, anti-NLRP3, anti-Caspase-1, and anti-ASC, all sourced from Proteintech (Wuhan, China). Anti-P62, anti-Beclin1, anti-Parkin, and anti-GAPDH antibodies, as well as HRP Goat Anti-Rabbit IgG, were supplied by Wanlei (China). DAPI staining solution and Alexa Fluor 488-conjugated goat anti-rabbit antibodies were provided by Servicebio (Wuhan, China). The Enhanced Chemiluminescence (ECL) kit was obtained from Biosharp (China).

Cell culture and cell viability assay

HT22 cells were cultured in the DMEM medium supplemented with 10% FBS and 1% penicillin-streptomycin and maintained at 37 °C in a 5% CO_2 atmosphere. Only cells in the exponential growth phase were used for all experiments.

For the experiments, 5×10^4 cells were seeded into each well of a 96-well plate and incubated at 37 °C. To determine the safe concentration of PF, 100 μL of PF solution at various concentrations (0, 1, 10, 50, 100, 200, 300, 400, and 500 μmol·L^{-1}) was administered to each well for 24 h. In a similar setup, wells were treated with 100 μL of CORT solution at concentrations ranging from 0 to 300 μmol·L^{-1} (0, 1, 5, 10, 20, 50, 100, 200, and 300 μmol·L^{-1}) for 24 h. Following the CORT treatment, cells were exposed to different concentrations of PF solution (0, 1, 10, 20, 50, 100, and 200 μmol·L^{-1}) for an additional 24 h. Cell viability was assessed using a CCK-8 assay. Briefly, 10 μL of CCK-8 solution was added to each well, and the absorbance was measured at a wavelength of 450 nm using an Epoch2 microplate reader (BioTek Instruments, Inc., USA) after 2 h of incubation at 37 °C. Cell viability (%) was calculated using the following formula: $(A_{drug} - A_{blank})/(A_{control} - A_{blank}) \times 100\%$.

Detection of mitochondrial reactive oxygen species (ROS)

Intracellular ROS levels were assessed using the fluorescent probe DCFH-DA. Initially, cells (1×10^5) were cultured in a 12-well plate and pretreated with 100 μmol·L^{-1} of CORT solution. This was followed by exposure to PF solution at concentrations of 50, 100, and 200 μmol·L^{-1} for 24 h. After treatment, the cells were washed twice with PBS and then incubated with 10 μmol·L^{-1} DCFH-DA for 30 min at 37 °C. Following the incubation, cells were washed three times with PBS to remove any residual probe. The fluorescence intensity of ROS was subsequently observed using a fluorescence microscope from Thermo Fisher Scientific.

Measurement of mitochondrial membrane potential (MMP)

Mitochondrial membrane potential (MMP) in HT22 cells was assessed using the fluorescent probe JC-1, a cationic dye that penetrates cell membranes and accumulates in mitochondrial aggregates in response to changes in MMP. Initially, HT22 cells were cultured at a density of 1×10^5 cells/ml in 12-well plates for 24 h. Following this incubation, the cells were washed once with PBS. JC-1 staining media was then added, and the cells were incubated at 37 °C for 20 min. After incubation, the cells were washed twice with JC-1 staining buffer, which was then discarded. A suitable amount of cell culture medium was added to each well, and the cells were subsequently observed under a fluorescence microscope (Thermo Fisher Scientific) to evaluate the MMP changes.

Detection of IL-6, IL-1β, IL-18 levels and caspase-1 activity in cells

To evaluate the anti-inflammatory effects of PF in HT22 cells, we measured the levels of inflammatory cytokines IL-1β, IL-18, and IL-6 in the HT22 cell culture medium using

enzyme-linked immunosorbent assay (ELISA) kits, following the manufacturer's instructions. Additionally, we quantified the content of Caspase-1 in the cell lysates using a Caspase-1 detection kit.

Animals

Adult male C57/BL6 mice weighing 18–23 g were obtained from Changchun Yisi Laboratory Animal Technology Co., Ltd.. The mice were housed under standardized conditions, maintained at 23 ± 2 °C and a relative humidity of 55% ± 5%. Throughout the experiment, the mice had free access to drinking water and a standard diet. After a week-long acclimatization period, the mice were randomly divided into seven groups (n = 8/group): Control, CUMS, CUMS + FLU (10 mg·kg^{-1}) [27], CUMS + PF (20 mg·kg^{-1}), CUMS + PF (40 mg·kg^{-1}), CUMS + PF (80 mg·kg^{-1}), and CUMS + PF (80 mg·kg^{-1}) + 3-MA (10 mg·kg^{-1}) [19]. All experimental procedures adhered to the animal experimentation guidelines of Jilin Agricultural University.

Animal experimental design

The CUMS treatment was conducted as previously described [28], with minor modifications to ensure the unpredictability of the stress protocol. The various stress modalities were randomly arranged, and no single stressor was repeated over three consecutive days. Stressors included (1) cage tilt (45°) for 12 h, (2) fasting for 12 h, (3) water fasting for 12 h, (4) ice water swimming (4 °C) for 5 min, (5) warm water swimming (28 °C) for 20 min (6) shaking the cage for 10 min, (7) reversing the light-dark cycle (overnight lighting, 12 h), (8) moist bedding for 12 h, (9) foreign body exposure for 12 h, (10) white noise for 6 h, (11) tail suspension for 10 min, and (12) heat stress for 5 min.

Mice not subjected to CUMS were housed in a separate room to prevent any interaction with the CUMS-exposed mice throughout the experiment. The animals underwent CUMS for 7 weeks. Starting from the fourth week, PF or FLU was administered *via* oral gavage daily. In addition, mice in the CUMS + PF + 3-MA group received daily intraperitoneal injections of 3-MA for seven consecutive days until the end of the experiment. Behavioral tests were conducted, and blood and brain tissues were collected for analysis after the experimental period. The experimental design is illustrated in Fig. 3A.

Behavioral testing

Sucrose preference test (SPT)

As previously noted, the SPT is used to assess anhedonia, a hallmark of depression, which manifests as a lack of pleasure [29]. To acclimate the mice to the taste of sucrose, two bottles containing 1% sucrose solution were introduced before the test. All animals underwent 24 h of fasting and water deprivation prior to the SPT. For the test, we prepared two pre-weighed bottles: one containing a 1% sucrose solution and the other containing sterile water. To minimize any positional bias, the location of each bottle was alternated every 2 h. After 4 h, the consumption from both the sucrose solution and the sterile water was recorded. Sucrose preference (100%) = sugar water consumption (sugar water consumption + pure water consumption) × 100%.

Tail suspension test (TST)

The degree of depression in mice was evaluated using the TST, which measures the immobility time as an indicator of depressive-like behavior. For the test, each mouse was suspended by the tail 50 cm above the floor. The total duration of the test was 6 min, with the first 2 min allocated for acclimatization, during which the mouse could adapt to the environment. The cumulative immobility time during the subsequent 4 min was then recorded. A mouse was considered immobile when it ceased showing movement while being passively suspended. All sessions were directly recorded using a camera to ensure accurate measurement of immobility times.

Forced swimming test (FST)

The FST was conducted to evaluate depressive-like behavior in mice. Each mouse was placed in a glass cylinder measuring 40 cm in height and 18 cm in diameter, filled with water to a height of 30 cm, and maintained at 23 ± 2 °C. The test lasted for 6 min, during which the first 2 min allowed for adaptation, and the immobility times were recorded during the subsequent 4 min. A mouse was considered immobile when it passively floated, making only minimal movements necessary to keep its head above water. All sessions were directly recorded with a camera to ensure precise documentation of the behavior.

Open field test (OFT)

The OFT is commonly employed to assess anxiety-like behaviors in mice [30]. The apparatus comprises an open-field reaction box and a camera connected to an analysis system. The reaction box, uncovered with black inner walls, measures 80 cm in length, width, and height. The floor of the box is divided into nine distinct active areas. During the test, two key behaviors were measured: the immobility time and the number of times a mouse crossed the center area, both recorded over a 5-minute period. The experiment was performed in a controlled, quiet environment. After each test, alcohol was used to clean the box thoroughly to remove feces and odors, preventing their effects on the results.

Elevated plus maze (EPM)

The EPM is commonly used to assess the effects of depression models and the efficacy of antidepressants. Prior to the experiment, the active area within the maze was defined. The behavior of the mice was recorded using cameras. For the test, each mouse was placed in the central area of the maze and allowed to move freely for 5 min. During this period, both the duration and trajectories within the open arms were recorded. The experiment was conducted in a quiet environment to minimize stress on the animals. To ensure consistency and cleanliness between sessions, continuous experiments were performed with different mice. After each session, feces were removed, and alcohol was used to clean the apparatus, eliminating odors that could potentially influence the experimental results.

Detection of IL-1β and CORT levels in serum and 5-HT and BDNF levels in the hippocampus

After the behavioral tests, blood samples were collected and centrifuged at 10 000 r·min^{-1} for 10 min at 4 °C to ob-

tain serum. Similarly, hippocampal tissue homogenates were centrifuged at 12 000 r·min^{-1} for 10 min at 4 °C to collect the supernatant. The levels of IL-1β and CORT in the serum and 5-HT and BDNF in the hippocampal tissue were measured using ELISA kits according to the manufacturer's instructions.

Hematoxylin-eosin (HE) staining

The pathological morphology of the hippocampus was evaluated using HE staining. Mouse hippocampal tissues were first fixed with 4% paraformaldehyde at room temperature. After fixation, the tissues were dehydrated in a series of alcohol solutions, embedded in paraffin, and then sectioned into 5 μm slices. The sections underwent HE staining, where they were initially stained with hematoxylin, rinsed, and then sequentially dehydrated in 70% and 90% alcohol solutions. Subsequently, the sections were stained with an eosin solution in alcohol. After staining, the sections were further dehydrated in absolute alcohol and cleared with xylene. An Olympus BX51 optical microscope was utilized to observe and capture images of the stained sections.

Transmission electron microscopy (TEM) analysis

The hippocampal tissues from mice in each group were sliced into sections (1–3 mm thick) and fixed by incubation in a solution of 2.5% glutaraldehyde and 2% paraformaldehyde at 4 °C for 2 h. After this initial fixation, the sections were further fixed with 1% osmium tetroxide. They were then treated with aqueous uranyl acetate, dehydrated through a graded series of alcohols, and embedded in epoxy resin. The sections were subsequently stained with lead citrate for enhanced contrast. Images of these prepared sections were captured using a transmission electron microscope (TEM, HITACHI HT7800, Japan).

Immunohistochemistry

After fixation, embedding, slicing, and dewaxing of the brain tissue, antigen retrieval was performed on the sections, which were then blocked to prevent non-specific binding. The sections were treated with 5% bovine serum albumin (BSA) for one hour. Following this, they were incubated overnight at 4 °C with primary antibodies targeting NLRP3, Caspase-1, and IL-1β. The sections were then incubated with the corresponding secondary antibodies. Staining was conducted using diaminobenzidine (DAB) to visualize the antigens. The stained sections were observed under an optical microscope and the density was quantitatively analyzed using Image-Pro Plus software.

Immunofluorescence

HT22 cells, seeded at a density of 1 × 10^5 cells/mL in a 12-well plate, underwent drug treatment before further processing. The cells were washed twice with PBS, fixed with 4% paraformaldehyde, permeabilized with 0.01% Triton X-100, and subsequently treated with 5% BSA to block non-specific binding. They were then incubated overnight with an anti-LC3 antibody, followed by a 1-hour incubation with Alexa Fluor 488-conjugated goat anti-rabbit antibody. DAPI staining was used for nuclear visualization.

Similarly, hippocampal sections were permeabilized with 0.5% Triton X-100 at room temperature for 20 min and blocked with normal goat serum for 30 min at room temperature. The sections were incubated overnight at 4 °C with anti-LC3 or anti-P62 antibodies, followed by a 1-hour incubation with Alexa Fluor 488-conjugated goat anti-rabbit antibody. DAPI was also used for nuclear re-staining in these sections. The images were captured using a BX53 fluorescence microscope, and the results were quantified using ImageJ software.

Western blotting analysis

Brain tissues and HT22 cells were lysed using RIPA buffer on ice for 30 min. The lysates were then centrifuged at 12 000 g for 10 min at 4 °C to separate the supernatants. Protein concentrations in the supernatants were determined using a BCA protein assay kit. Proteins were separated on a 12% sodium dodecyl sulfate-polyacrylamide gel electrophoresis (SDS-PAGE) and subsequently transferred to PVDF membranes. These membranes were blocked with 5% skim milk in TBST for 1 hour at room temperature, then incubated with the appropriate primary antibodies overnight at 4 °C. After washing, the membranes were incubated with secondary antibodies for 1 hour. Protein bands were visualized using enhanced chemiluminescence with a Chemiluminescence Imager (Analytik Jena). Quantitative analysis of the protein expression was performed using ImageJ software.

Graphing and statistical analysis

All data were presented as mean ± standard deviation. Statistical analyses were conducted using one-way analysis of variance (ANOVA), with Tukey's test employed for comparisons between multiple groups. Values of $P < 0.05$ were considered statistically significant. The statistical analyses were performed using SPSS software version 20.0, and graphs were generated with GraphPad Prism 8 (GraphPad Software, Inc., La Jolla, CA, USA).

Results

Effect of PF on the viability of CORT-induced HT22 cells

As depicted in Fig. 1B, cell viability began to increase at a PF concentration of 10 μmol·L^{-1} and remained non-cytotoxic across a range of 1–500 μmol·L^{-1}, peaking at a PF concentration of 200 μmol·L^{-1}. In contrast, as shown in Fig. 1C, cell viability decreased in a dose-dependent manner following CORT induction. Notably, cell viability approached 50% at a CORT concentration of 100 μmol·L^{-1}, which was therefore selected for further experiments. In the CORT-induced HT22 cell model, various concentrations of PF were evaluated for their therapeutic effects. Fig. 1D illustrates that the highest cell viability was observed at a PF concentration of 200 μmol·L^{-1}. Consequently, concentrations of 50, 100, and 200 μmol·L^{-1} were chosen for subsequent experiments.

Effects of PF on ROS production and mitochondrial function in CORT-induced HT22 cells

Mitochondrial damage can lead to increased expression of reactive oxygen species (ROS), which serve as indicators of such damage. Intracellular ROS levels were measured using the non-fluorescent probe DCFH-DA, which, when oxid-

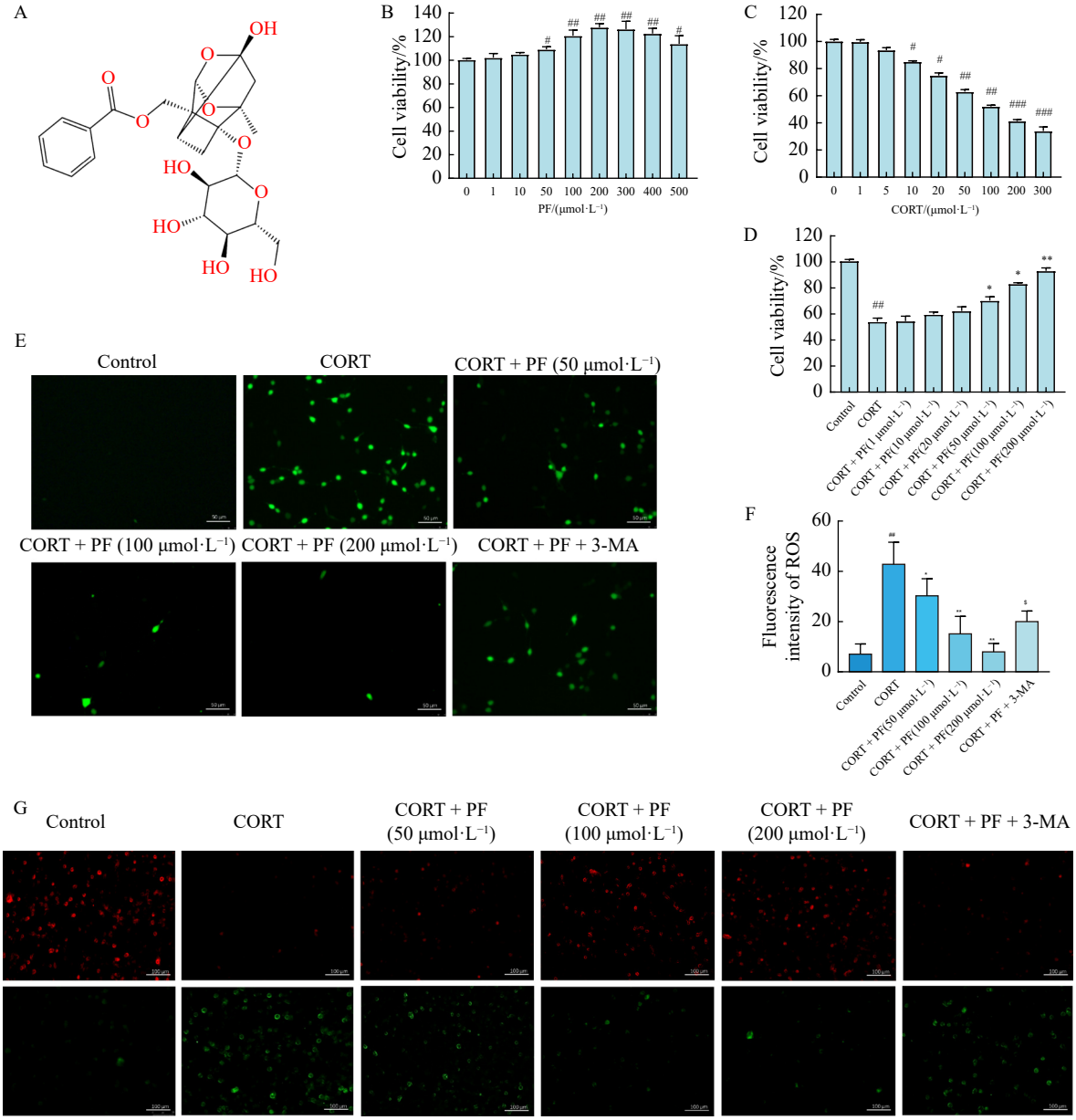

Fig. 1 Effect of PF on HT22 cell viability, ROS production, and mitochondrial function. (A) The chemical structure of PF. (B–D) Cytotoxic effects of PF and CORT at different concentrations on HT22 cells and that of PF on CORT-induced cells using the CCK-8 assay. (E, F) The expression of ROS in HT22 cells after staining with HDCF-DA (10 μmol·L^{-1}) was captured under a fluorescence microscope. (G) The JC-1 fluorescence of cells was observed by fluorescence microscopy to assess the MMP of cells. The values were represented as the mean ± SD, $n = 8$. $^{\#}P < 0.05$, $^{\#\#}P < 0.01$, $^{\#\#\#}P < 0.001$ *vs* the control group; $^{*}P < 0.05$, $^{**}P < 0.01$ *vs* the CORT group.

ized, becomes the fluorescent DCF. Fig. 1E and Fig. 1F illustrate that CORT-treated cells exhibited stronger DCF fluorescence compared to the control group. Following treatment with PF, the fluorescence intensity decreased in a dose-dependent manner, indicating that PF effectively inhibits CORT-induced ROS production.

Mitochondrial membrane potential (MMP) was assessed using fluorescence microscopy to evaluate the extent of mitochondrial damage. This was monitored using JC-1 staining, where red-fluorescent JC-1 aggregates indicate highly polarized membranes and green fluorescent monomeric forms signal membrane depolarization. A higher integrity of the mitochondrial membrane is reflected by a greater ratio of red to green fluorescence. As shown in Fig. 1G, PF treatment restored MMP and mitochondrial membrane integrity, thereby mitigating CORT-induced mitochondrial damage.

Effects of PF on the expression of Inflammatory cytokine, NLRP3 and LC3, in HT22 cells

To evaluate the effects of PF *in vitro*, we analyzed the levels of inflammatory cytokines secreted by cell cultures. Results shown in Figs. 2A–2C indicate that CORT induced the release of IL-6, IL-1β, and IL-18 compared to the control

group. Conversely, PF treatment significantly reduced the CORT-induced levels of these cytokines in HT22 cells in a dose-dependent manner. Further analysis focused on the role of PF in modulating NLRP3 inflammasome activity; we examined the expression of NLRP3 and caspase-1 in cells treated with the autophagy inhibitor 3-MA for additional validation [27]. Fig. 2D illustrates that PF treatment notably restored the expression of caspase-1 in cell lysates relative to the CORT group. Western blot analysis revealed that PF treatment increased the protein expression level of LC3 and decreased the expression of NLRP3 compared to the model group. However, these effects were partially reversed following treatment with the 3-MA inhibitor, as evidenced in Figs. 2E–2G. Furthermore, we assessed the expression levels of the autophagy marker LC3 using immunofluorescence staining. Fig. 2H demonstrates that the fluorescence intensity of LC3 was significantly lower in the model group than in the control group, whereas PF treatment enhanced LC3 fluorescence in CORT-induced HT22 cells. These findings suggest that PF mitigates the release of inflammatory cytokines and

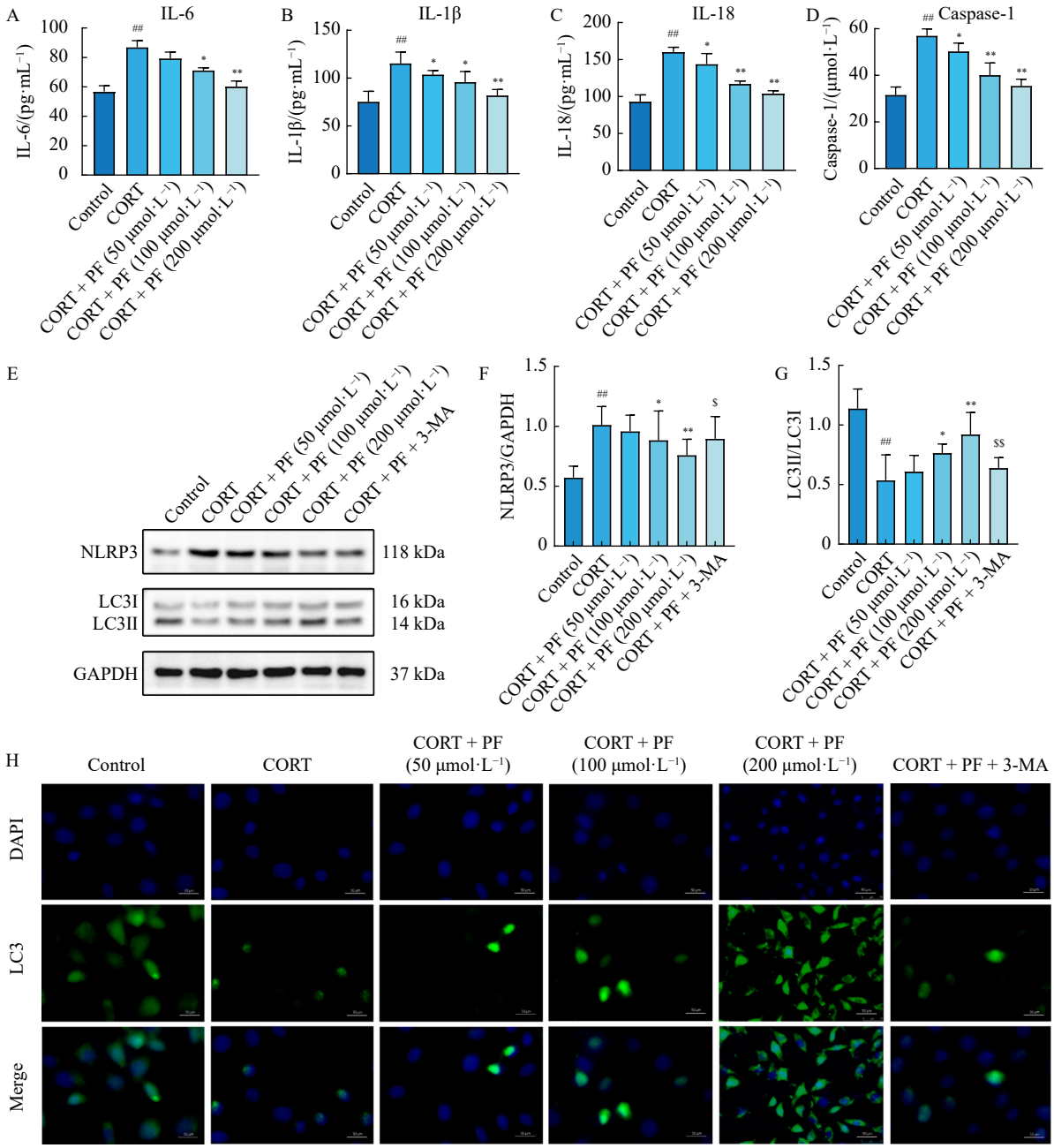

Fig. 2 Effect of PF on the expression of Inflammatory cytokine, NLRP3 and LC3 in HT22 cells. (A–C) The levels of IL-6, IL-1β, and IL-18 in HT22 cells. (D) The expression of Caspase-1 in cell lysates. (E–G) The protein expression levels of LC3 and NLRP3. (H) The fluorescence intensity of LC3 (green) in HT22 cells was observed by LC3/DAPI staining. All data are expressed as mean ± S.D, $n = 8$. $^{\#\#}P < 0.01$ *vs* the control group. $^{*}P < 0.05$, $^{**}P < 0.01$ *vs* the CUMS group.

the expression of NLRP3, and it restores LC3 expression in CORT-treated HT22 cells. This protective effect of PF may be attributed to its anti-inflammatory and mitochondrial autophagy-enhancing properties.

Effect of PF on depression-like behavior in CUMS model mice

FLU, a widely recognized selective serotonin reuptake inhibitor, is commonly used in the clinical treatment of depression [31]. In this study, a mouse model of depression was established using chronic unpredictable mild stress (CUMS), followed by treatment with PF at doses of 20, 40, and 80 $mg \cdot kg^{-1} \cdot d^{-1}$ or FLU at a dose of 20 $mg \cdot kg^{-1} \cdot d^{-1}$, administered intragastrically for four weeks (Fig. 3A). After three weeks, there was a significant decrease in both body weight and sucrose preference in the CUMS-exposed mice compared to the control group. However, both PF and FLU treatment gradually reversed these effects, with significant increases in body weight and sucrose consumption observed at the end of the 6th and 7th weeks of treatment (Figs. 3B, 3C). Additionally, PF administration significantly reduced the immobility time in the FST and the TST in a dose-dependent manner, indicating an antidepressant effect (Figs. 3D, 3E).

The OFT and EPM also demonstrated the efficacy of PF and FLU treatments. Both treatments significantly decreased immobility time in the OFT and increased the time spent in the central area (Figs. 3F, 3G). Similarly, thermographic analysis showed improved behavior in the PF- or FLU-treated mice compared to the CUMS group, indicating a reduction in depressive-like behaviors (Fig. 3J). In the EPM, the CUMS group showed significantly less time spent in the open arms and fewer entries into these arms compared to the control group. Treatment with FLU and PF markedly increased both the time spent and the number of entries into the open arms compared to the CUMS group (Figs. 3H, 3I), further substantiating their antidepressant effects. Overall, these results confirm that both PF and FLU effectively reduce the symptoms of depression in CUMS-induced mice (Fig. 3K).

Levels of BDNF, 5-HT, CORT and IL-1β in CUMS mice

BDNF is a crucial neurotrophic protein abundantly found in brain tissue. It plays a vital role in neuronal growth, differentiation, and synaptic activity and is acknowledged for its involvement in various psychiatric disorders, including major depression [32]. Depression is often linked with imbalances in key monoamine neurotransmitters such as 5-HT in the brain [33]. Following treatment with PF, both BDNF and 5-HT levels in the hippocampus were observed to increase in a dose-dependent manner when compared to the CUMS group. CORT, a glucocorticoid produced by the adrenal cortex, plays a pivotal role in regulating the HPA axis and is frequently studied in clinical research on depression. Emerging evidence suggests a significant association between depression and inflammation, highlighting their potential interactions [34]. Fig. 4A demonstrates that both CORT and the inflammatory cytokine interleukin-1β (IL-1β) were markedly elevated in the model group compared to the control group. Importantly, these levels significantly decreased in a dose-dependent manner following administration of PF, underscoring its potential anti-inflammatory and therapeutic effects in the context of depression.

Analysis of histopathological examination

HE staining revealed that in the control group, hippocampal neuronal cells were neatly and closely arranged with normal intercellular gaps and intact morphology and structure. In contrast, the hippocampal neuronal cells in the model group showed significant deficiencies, characterized by sparse and disorganized cell arrangement, vacuolated cytosol, deeply stained nuclei, and pronounced changes in cell morphology and structure. Notably, these signs of hippocampal damage in the model mice were alleviated following treatment with PF, with the most substantial improvements observed at higher doses (Fig. 4B).

Effect of PF on mitochondrial damage and autophagosomes production in CUMS mice

To investigate the ultrastructure of the hippocampus and the activation of autophagy, we utilized TEM to observe the morphology of mitochondria in the hippocampal cells of mice. The TEM analysis revealed that compared with that in the control group, the mitochondria in the CUMS group were significantly damaged. This damage was characterized by morphological and structural changes, including swelling, vacuolation, and shortening of mitochondrial cristae, as indicated by yellow arrows. Conversely, treatment with FLU and PF at doses of 40 and 80 $mg \cdot kg^{-1}$ effectively cleared the damaged mitochondria and restored their normal morphology. Additionally, TEM analysis showed that, compared to the control group, there was no significant accumulation of autophagosomes in the model group. Most notably, several autophagosomes, marked by red arrows, were observed in the cytoplasm of cells treated with PF and FLU. This finding indicates that PF treatment can promote the fusion of cytoplasmic components with lysosomes, thereby activating autophagy and leading to the formation of autophagosomes (Fig. 4C).

Effect of PF on the activation of NLRP3 pathway in the hippocampus

To explore the role of the NLRP3 inflammasome in the antidepressant mechanism of PF, we analyzed the expressions of NLRP3, ASC, Caspase-1, and IL-1β. The results indicated that, compared to the control group, the protein expressions of NLRP3, ASC, Caspase-1, and IL-1β were significantly upregulated in the CUMS group, demonstrating activation of the NLRP3 inflammasome. However, both PF and FLU treatment significantly decreased the expressions of these proteins in the hippocampus of CUMS-induced mice (Figs. 5A, 5B). Additionally, immunohistochemical staining was employed to specifically assess NLRP3 expression in the hippocampus. This analysis revealed that CUMS significantly increased the positive signal intensity of NLRP3 in the hippocampus. In contrast, PF administration notably inhibited the activation of NLRP3, further substantiating its potential role in mitigating depressive behaviors by modulating inflammatory pathways (Figs. 5C, 5D).

Effect of PF on autophagy activation in the hippocampus

We further investigated the antidepressant mechanism of

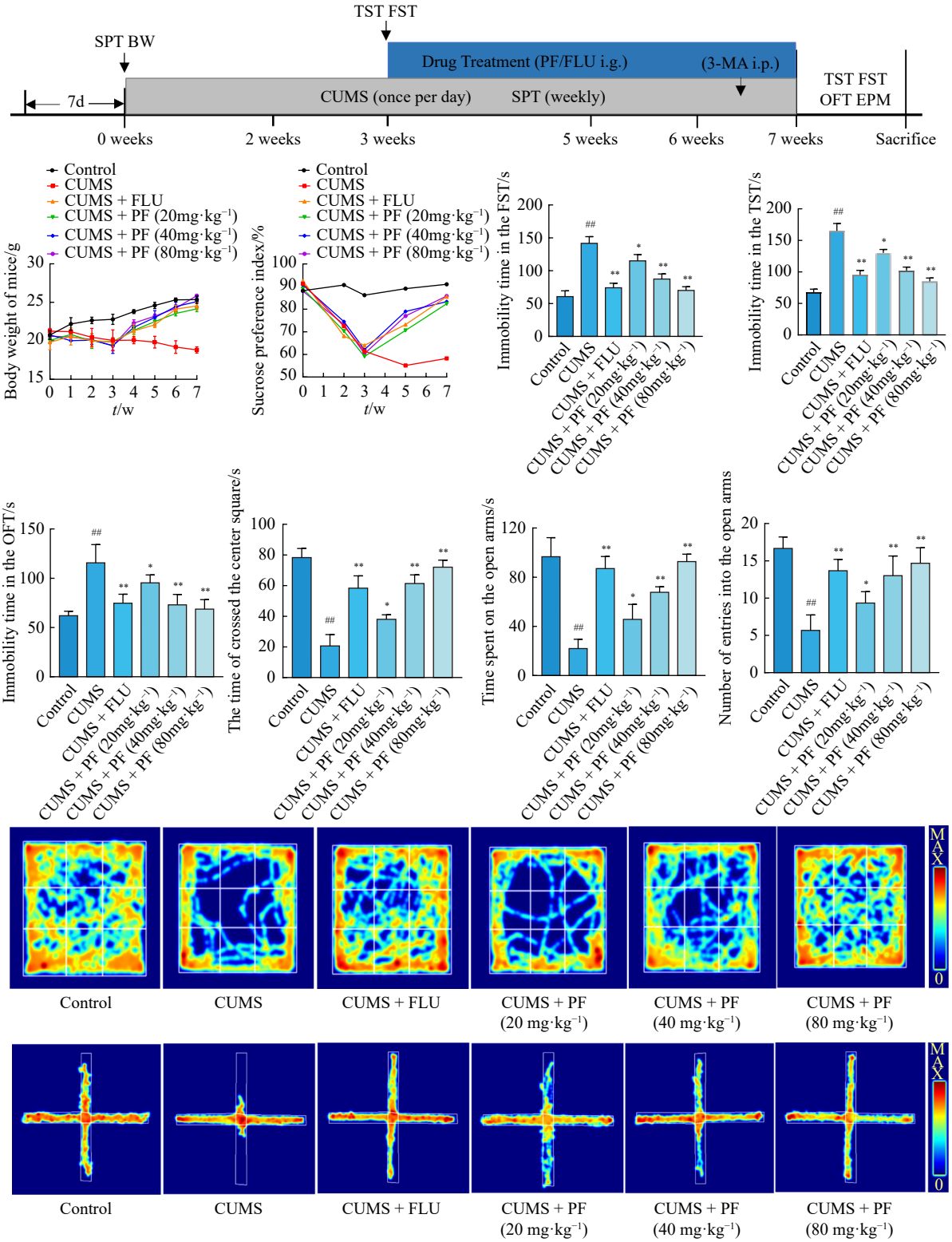

Fig. 3 Effect of PF on depression-like behavior in CUMS model mice. (A) The program of CUMS model preparation and drug administration in the present study. (B, C) The effects of PF on body weight and sucrose consumption of CUMS-induced depression mice. (D, E) The effects of PF on the immobility time of mice in TST and FST. (F, G) The effect of PF on immobility time and time crossed the central square in OFT. (H, I) The effect of PF on open arms and the number of entries into the open arm in EPM. (J) The activity thermograms of mice in OFT. (K) The activity thermograms of mice in EPM. The values were represented as the mean ± SD, $n = 8$. $^{\#\#}P < 0.01$ *vs* the control group. $^{*}P < 0.05$, $^{**}P < 0.01$ *vs* the CUMS group.

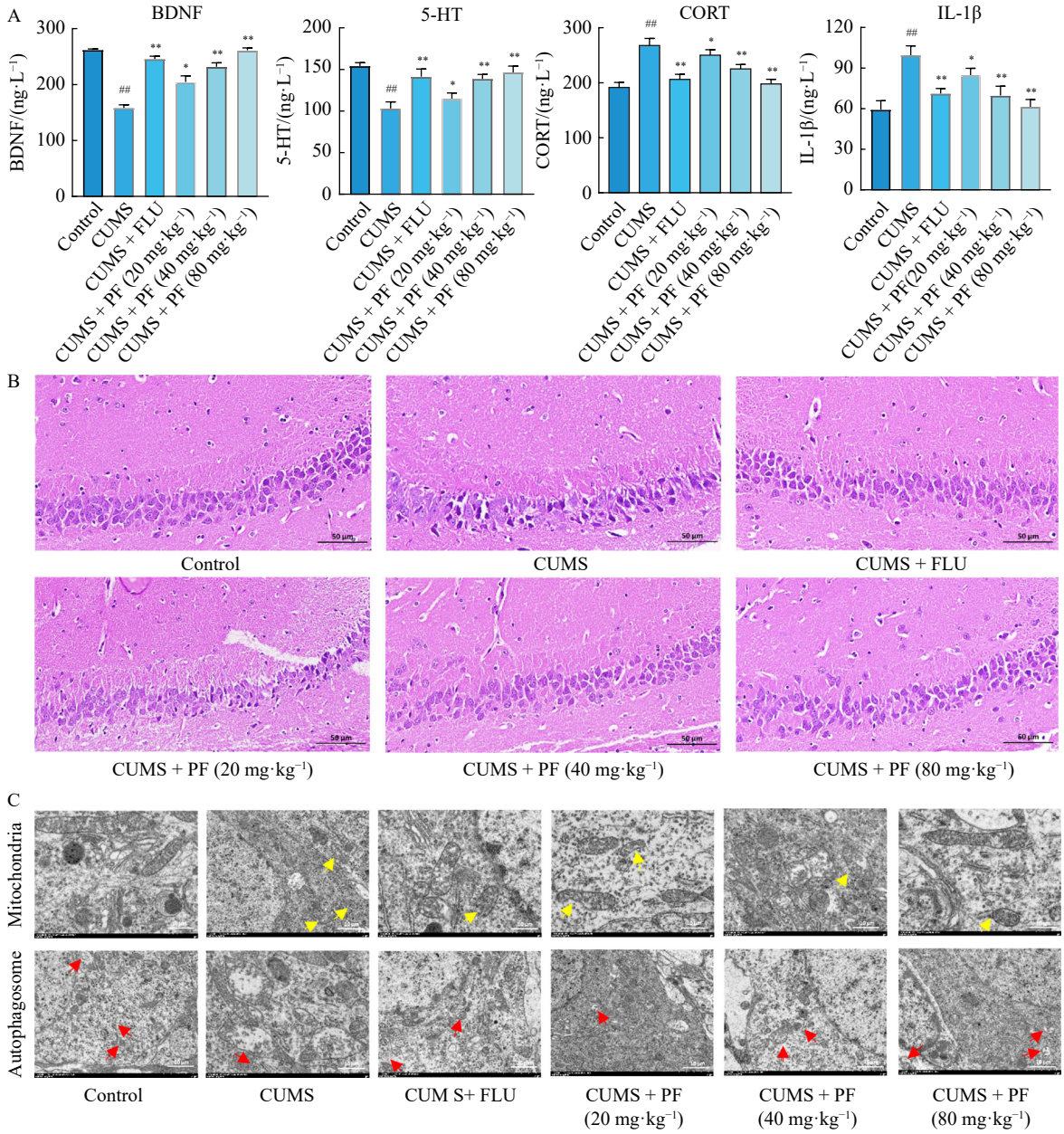

Fig. 4 Effects of PF on BDNF, 5-HT, CORT, and IL-1β levels, histopathological examination, and mitochondrial morphology and autophagosomes in CUMS mice. (A) The levels of IL-1β and CORT in serum and the levels of 5-HT and BDNF in hippocampal neurons were assessed by ELISA. (B) The pathological damage of hippocampal neurons was evaluated by HE staining. (C) Images of damaged mitochondria (yellow arrow) and autophagosomes (red arrows) were observed by transmission electron microscopy. The values were represented as the mean ± SD, $n = 8$. $^{\#\#}P < 0.01$ *vs* the control group. $^{*}P < 0.05$, $^{**}P < 0.01$ *vs* the CUMS group.

PF by examining the expression levels of autophagy-related proteins. Western blot analysis revealed significant abnormalities in autophagy in the CUMS group compared to the control group. Specifically, there was a decrease in the ratio of the autophagy marker LC3II to LC3I, an increase in the expression level of the autophagy substrate P62, and decreased expression levels of the autophagy-related proteins Beclin1 and Parkin. However, treatment with PF or FLU normalized these protein expression levels, bringing them close to those observed in the control group (Fig. 6A, 6B). Additionally, LC3/DAPI staining of the hippocampus further confirmed the abnormal expression of LC3 in the hippocampus of the model group. This abnormal expression was corrected following treatment with PF or FLU (Fig. 6C). These findings suggest that the therapeutic effects of PF may be mediated through the activation of autophagy pathways.

PF inhibits NLRP3 synthesis by promoting the activation of mitochondrial autophagy in the hippocampus

To confirm the neuroprotective effects of PF by promoting mitochondrial autophagy in the hippocampus, we admin-

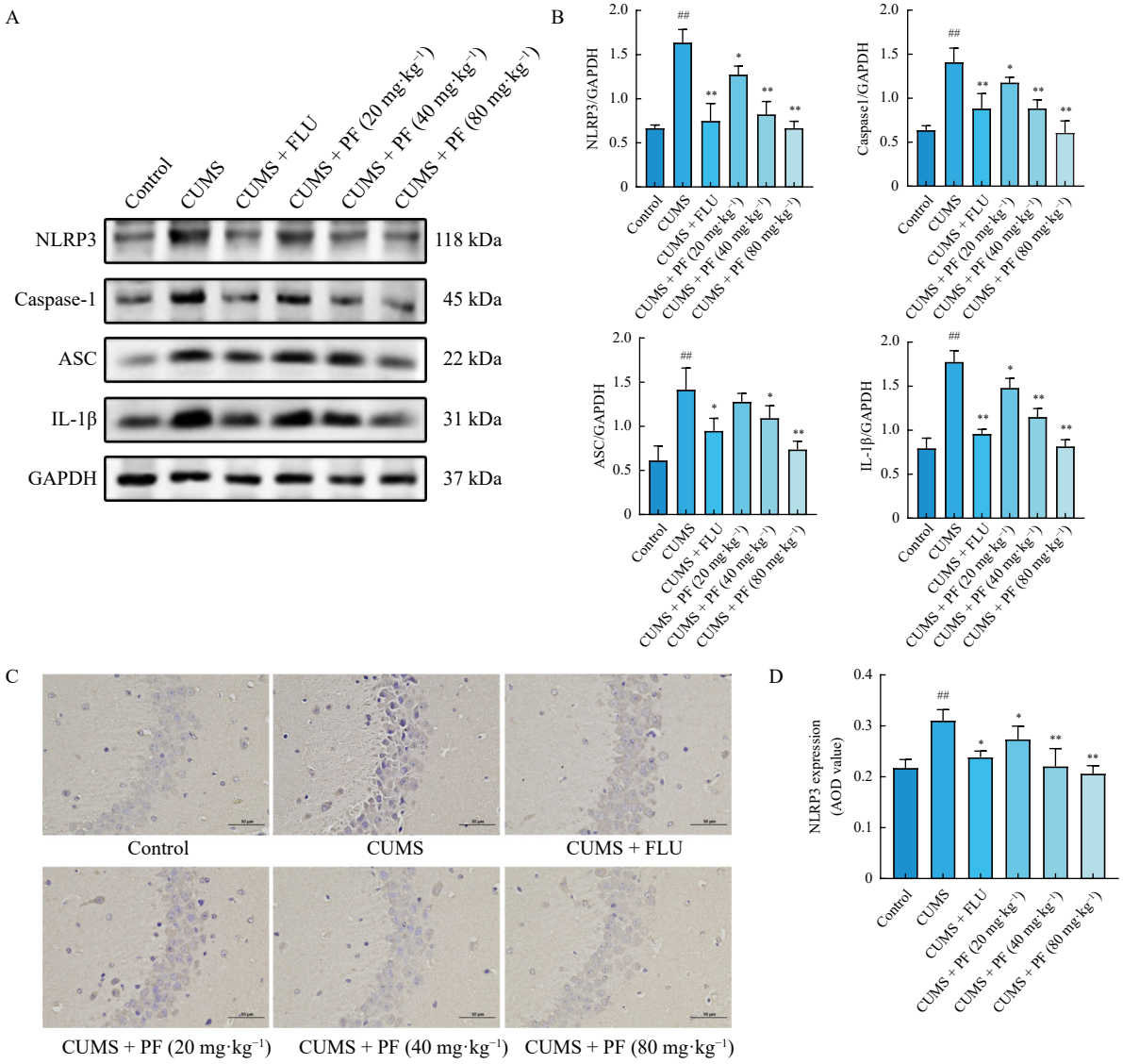

Fig. 5 The effect of PF on the activation of the NLRP3 pathway in the hippocampus. (A, B) The protein expressions of NLRP3, Caspase-1, ASC, and IL-1β in the hippocampus were determined by Western blot analysis. Quantitative analysis was performed by densitometry. (C, D) The expression NLRP3 in the hippocampus was observed by IHC staining. The values were represented as the mean ± SD, $n = 8$. $^{\#\#}P < 0.01$ *vs* the control group. $^{*}P < 0.05$, $^{**}P < 0.01$ *vs* the CUMS group.

istered 3-MA, an autophagy inhibitor, intraperitoneally to mice in the CUMS + PF + 3-MA group for one week before the end of the experiment. In hippocampal slices from the CUMS group, mitochondria (indicated by yellow arrows) appeared damaged. This damage was alleviated after PF treatment. Notably, we observed several autophagosomes (marked by red arrows) located near the mitochondria in the cytoplasm of the CUMS + PF group. However, in the CUMS + PF + 3-MA group, the damaged mitochondria were not cleared, and no obvious autophagosomes were observed, suggesting that the autophagy activated by PF was inhibited by 3-MA (Fig. 7A). Western blotting results further supported these findings, showing that PF decreased the expression of P62 and enhanced the expression of LC3, Parkin, and Beclin1. However, these effects of PF were attenuated by 3-MA treatment (Figs. 7B and 7C). Immunofluorescence staining results corroborated these observations, indicating that the relative fluorescence intensity of LC3, an autophagy marker, was increased after PF treatment, while the fluorescence intensity of P62, an autophagy substrate, was decreased compared to the CUMS group. This effect was reversed following 3-MA treatment (Figs. 7D and 7E). These results highlight the role of autophagy in the neuroprotective mechanism of PF in treating depression-induced hippocampal damage.

The results from both Western blotting and immunohistochemistry (IHC) staining substantiated our initial hypotheses. The autophagy inhibitor 3-MA effectively negated the suppressive impact of PF on the expression of NLRP3, Caspase-1, ASC, and IL-1β within the hippocampus (Figs. 8A and 8B). Similarly, the reduction in positive signal intensity of NLRP3, Caspase-1, and IL-1β, facilitated by PF, was reversed upon treatment with 3-MA (Figs. 8C–8F). These ob-

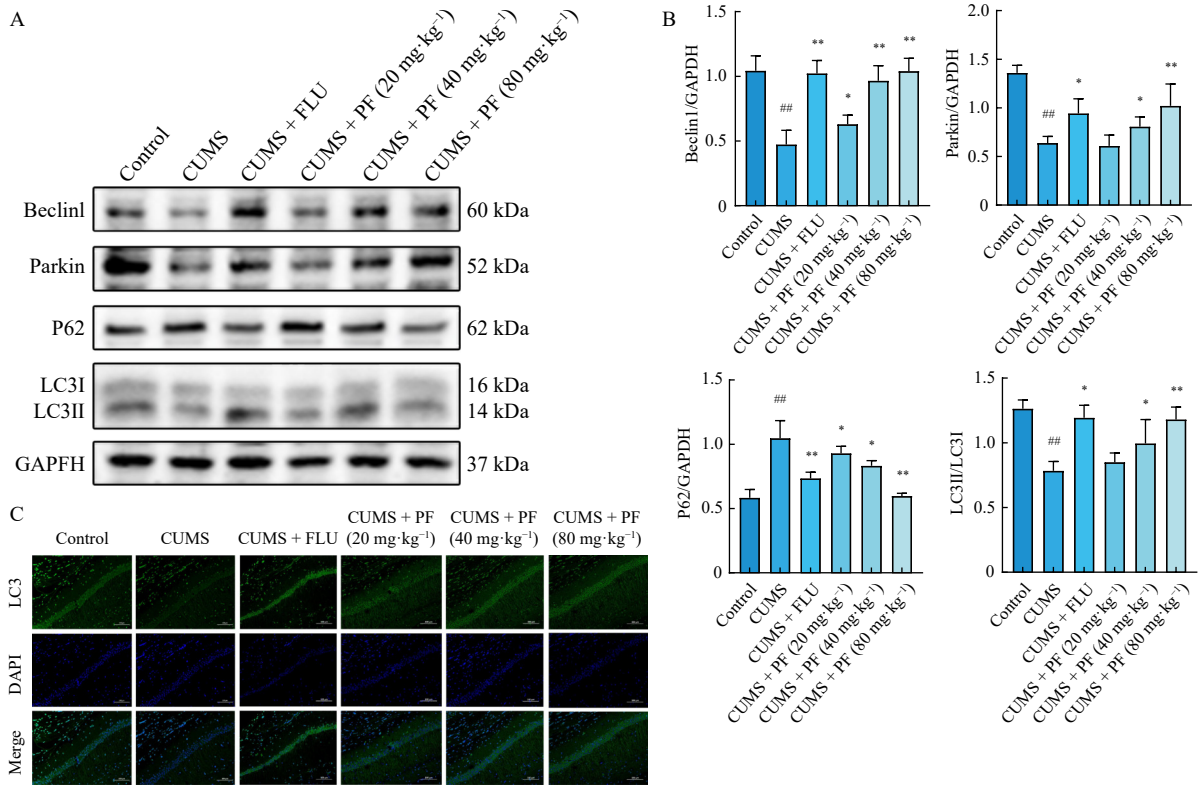

Fig. 6 Effect of PF on the expression of autophagy marker LC3 in the hippocampus. (A, B) The expressions of Beclin1, Parkin, P62, and LC3 in the hippocampus were determined by Western blot analysis. Quantitative analysis was performed by densitometry. (C) Fluorescence intensity of LC3 (green) in the hippocampus was observed by LC3/DAPI staining. The values were represented as the mean ± SD, $n = 8$. $^{\#\#}P < 0.01$ *vs* the control group. $^{*}P < 0.05$, $^{**}P < 0.01$ *vs* the CUMS group.

servations indicate that PF can confer neuroprotective and antidepressant effects by inhibiting the activation of the NLRP3 inflammasome in a CUMS-induced depression model in mice. This effect is likely mediated through the activation of autophagy within the hippocampus.

Discussion

PF is a naturally occurring monoterpene glycoside that has garnered attention for its neuroprotective properties, ability to promote autophagy, and potential to mitigate neuroinflammation. Despite these attributes, the linkage between PF's antidepressant effects and its influence on the interaction between autophagy and the NLRP3 inflammasome remains underexplored. This study aims to elucidate the antidepressant mechanisms of PF, specifically through the activation of autophagy and the inhibition of inflammation induced by CORT in HT22 cells *in vitro* and in CUMS model mice *in vivo*.

CORT, a corticosteroid produced by the adrenal cortex, has been shown to impair the morphology and function of hippocampal neurons when elevated. To model these effects, we established a CORT-induced HT22 cell model to simulate neuroinflammation and hippocampal neuronal damage *in vitro*. Accumulation of ROS can trigger the activation of the NLRP3 inflammasome, leading to an inflammatory response [35]. Our findings indicate that CORT exposure suppresses HT22 cell proliferation, elevates ROS expression, diminishes mitochondrial function, and decreases LC3 expression levels. Additionally, CORT was observed to increase the secretion of inflammatory cytokines IL-6, IL-1β, and IL-18, and to enhance the expression of NLRP3 and Caspase-1. As hypothesized, these adverse effects were ameliorated by high concentrations of PF. This reversal was further substantiated through the application of the autophagy inhibitor 3-MA, confirming the critical role of autophagy in the therapeutic action of PF.

The etiology and pathophysiological mechanisms underlying CUMS are analogous to those observed in human depression. In mice subjected to CUMS, PF ameliorated depression-like behaviors, as evidenced by improvements in the SPT, FST, TST, OFT, and EPM. These results underscore PF's potential efficacy in treating depression. The study also sought to elucidate whether PF influences autophagy regulation and NLRP3 inflammasome synthesis. Emerging evidence indicates that multiple inflammatory cytokines play significant roles in the pathogenesis of depression [36], steering new research directions toward anti-inflammatory therapies for its prevention and treatment [37]. Recent studies corroborate that inflammatory responses are markedly heightened in both depressed patients and animal models [38]. In alignment with these observations, our study revealed significant reductions in BDNF and 5-HT levels in the hippocampus of CUMS mice, alongside increased IL-1β expression in the serum. HE

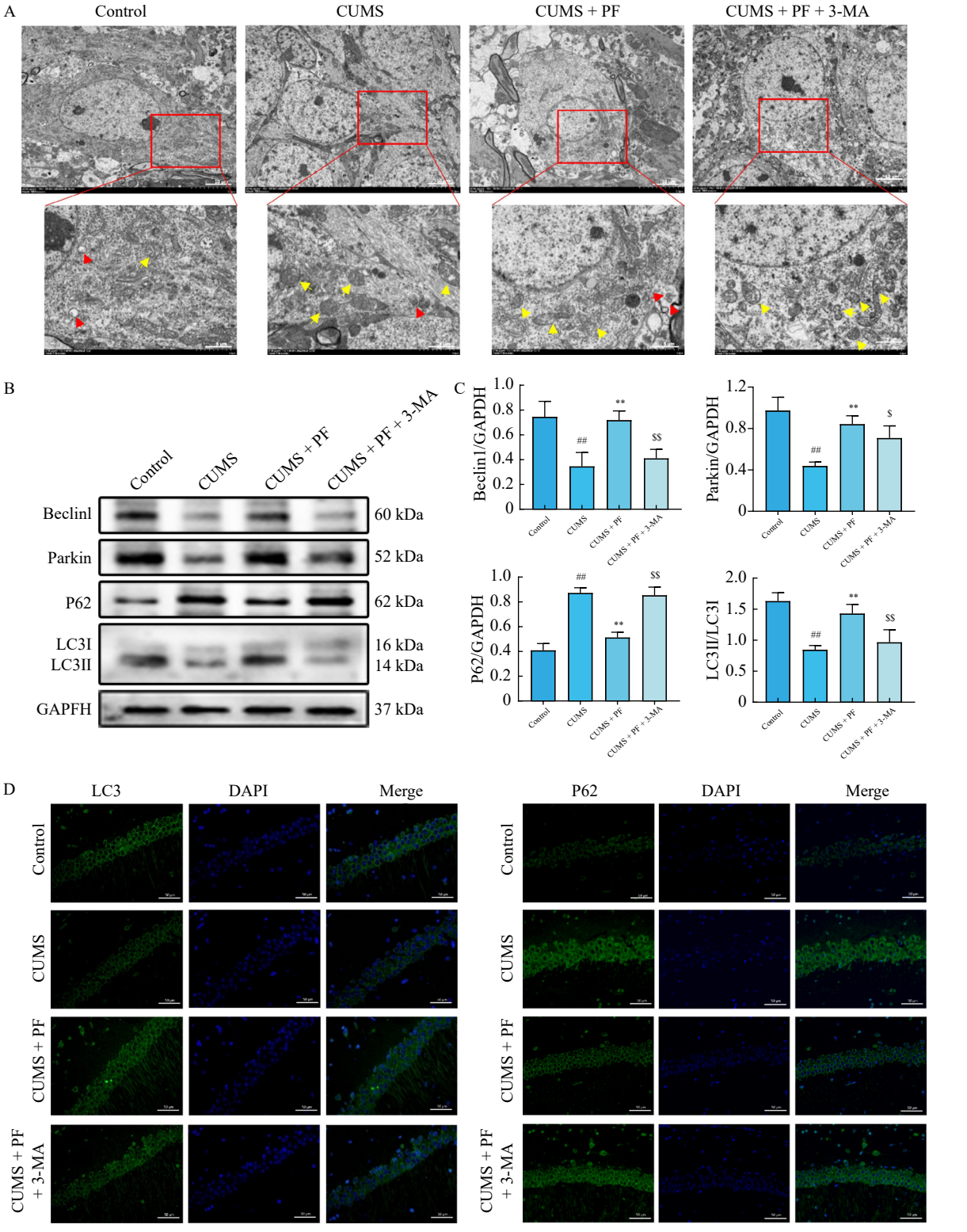

Fig. 7 Effect of 3-MA on the promotion of mitochondrial autophagy by PF. (A) Images of damaged mitochondria (yellow arrows) and autophagosomes (red arrows) were observed by transmission electron microscopy. (B, C) The protein expressions of Beclin1, Parkin, P62, and LC3 in the hippocampus were determined by Western blot analysis. Quantitative analysis was performed by densitometry. (D, E) Fluorescence intensity of LC3, and P62 (green) in the hippocampus observed by immunofluorescence staining. The values were represented as the mean ± SD, n = 8. $^{\#\#}P < 0.01$ *vs* the control group. $^{*}P < 0.05$, $^{**}P < 0.01$ *vs* the CUMS group. $^{\$}P < 0.05$, $^{\$\$}P < 0.01$ *vs* the PF group.

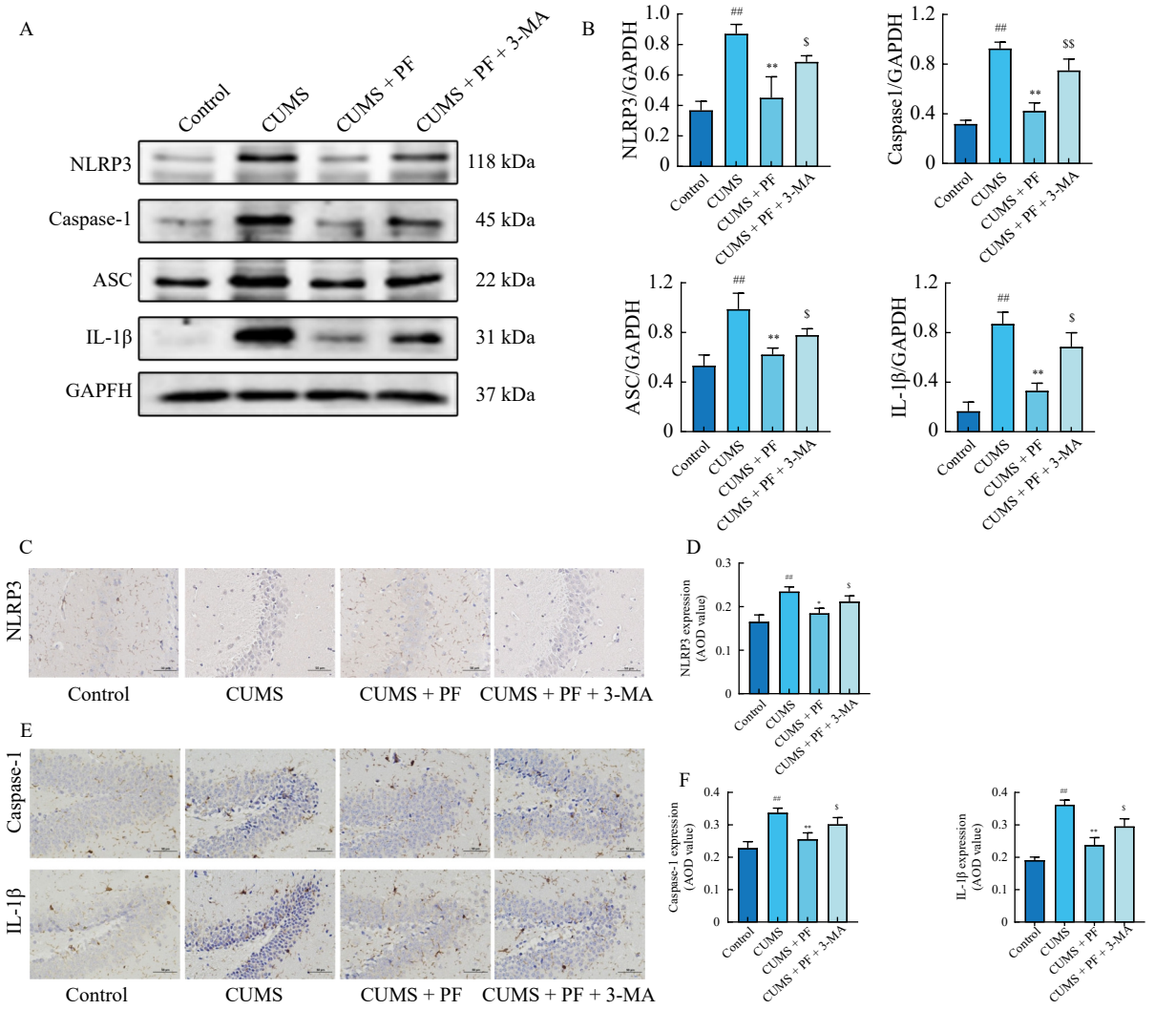

Fig. 8 Effect of 3-MA on the inhibitory effect of PF on the activation of the NLRP3 inflammasome. (A, B) The protein expressions of NLRP3, Caspase-1, ASC, and IL-1β in the hippocampus were determined by Western blot analysis. Quantitative analysis was performed by densitometry. (C, D) The expression of NLRP3 in the hippocampus was observed by IHC staining. (E, F) The expression of Caspase-1 and IL-1β in the hippocampus was observed by IHC staining. The values were represented as the mean ± SD, $n = 8$. $^{\#\#}P < 0.01$ *vs* the control group. $^{*}P < 0.05$, $^{**}P < 0.01$ *vs* the CUMS group, $^{\$}P < 0.05$, $^{\$\$}P < 0.01$ *vs* the PF group.

staining also highlighted inflammation within the hippocampus of CUMS mice, with these adverse effects being substantially mitigated following PF treatment. These findings suggest that PF's antidepressant action may be partially due to its capacity to inhibit inflammation, potentially through the modulation of the NLRP3 inflammasome.

When exposed to external stimuli, an inflammatory response is triggered, and defective, unwanted, or aged mitochondria produce toxic byproducts, particularly ROS, which pose a threat to themselves, adjacent mitochondria, and host cells. Autophagy serves as a cellular mechanism for degrading organelles and invading pathogens. During this process, autophagosomes and lysosomes fuse to form autophagic lysosomes, releasing lysosomal hydrolases that degrade the encapsulated mitochondria and facilitate the formation of autophagosomes. Subsequently, damaged mitochondria are cleared through mitochondrial autophagy. Transmission electron microscopy has revealed significant alterations in the morphology of mitochondria in the hippocampi of mice subjected to CUMS, indicating mitochondrial damage. Treatment with varying doses of PF has demonstrated the capability to either remove or repair these damaged mitochondria. Notably, after treatment with PF, a small number of autophagosomes were observed, with the highest levels present in the high-dose group. The autophagy inhibitor 3-MA counteracted this effect by inhibiting the autophagy-promoting actions of PF. Therefore, PF can effectively remove damaged mitochondria from the hippocampus of CUMS-induced mice, repair mitochondrial dysfunction, and promote the formation of autophagosomes. This suggests that PF may provide a therapeutic approach to mitigating mitochondrial damage and enhancing cellular resilience in the context of stress-induced depressive states.

Research has indicated that promoting autophagy can in-

hibit NLRP3 inflammasome activation and subsequently mitigate inflammatory responses [39]. To further elucidate the antidepressant mechanisms of PF, this study investigated its effects on NLRP3 inflammasome activity *in vivo*. Results demonstrated that PF significantly reduced the expression levels of NLRP3 in the hippocampus of mice subjected to CUMS. Additionally, Western blot analysis revealed that PF attenuated the activation of the inflammasome in the hippocampus by decreasing the expression of key components, including NLRP3, ASC, Caspase-1, and IL-1β. Combined with findings from *in vitro* studies, our data suggest that PF may exert anti-inflammatory and neuroprotective effects by inhibiting ROS production and suppressing NLRP3 inflammasome activation. These mechanisms underscore PF's potential therapeutic efficacy in treating depression, highlighting its significance for further clinical investigations.

When mitochondria are exposed to external stimuli, such as oxidative stress, PINK1 accumulates on the mitochondrial outer membrane via the outer membrane translocation enzyme, activating and recruiting Parkin. Parkin then ubiquitinates proteins on the mitochondrial outer membrane, which initiates mitochondrial autophagy. Following ubiquitination, receptor proteins including p62 accumulate on the outer mitochondrial membrane, facilitating the recruitment of ubiquitinated products to the autophagosome by binding to LC3. Mature autophagosomes subsequently fuse with lysosomes, forming autolysosomes that degrade their contents. Beclin1, a key protein in autophagy regulation, has recently been identified as instrumental in this process. Our findings demonstrate that PF enhanced the fluorescence intensity of LC3 and reduced that of P62 in the hippocampi of mice subjected to CUMS. Western blot analysis also indicated that PF increased the expression levels of Beclin1, Parkin, and the LC3II/LC3I ratio while decreasing the expression of P62 in the hippocampus of CUMS-induced mice. These effects were reversed following intervention with the autophagy inhibitor 3-MA, which interestingly increased the expression and fluorescence intensity of NLRP3 and related proteins, contrasting with PF's effects. These results suggest that PF inhibits the activation of the NLRP3 inflammasome and its associated inflammatory response by activating autophagy.

Taken together, the mitochondrial damage and activation of the NLRP3 inflammasome induced by external stimuli led us to hypothesize that promoting autophagy and clearing damaged mitochondria could inhibit the activation of the NLRP3 inflammasome. We provided compelling evidence that PF exerts neuroprotective and antidepressant effects by inhibiting NLRP3 inflammasome activation and reducing ROS production through the induction of mitochondrial autophagy (Fig. 9). Investigating the potential mechanisms underlying the inhibitory effects of PF on external stress-induced inflammatory responses may offer new insights and strategies for promoting PF as a therapeutic agent for depression.

Conclusion

In conclusion, PF has been shown to effectively inhibit inflammatory reactions both *in vivo* and in *vitro,* with these effects seemingly mediated by PF-induced autophagy. Therefore, the enhancement of autophagy alongside the inhibition of NLRP3-mediated inflammation likely constitutes the core mechanisms underlying the antidepressant effects of PF. These findings propose that a dual-targeted therapeutic approach—promoting mitochondrial autophagy while simultaneously suppressing inflammation —may be more effective than strategies targeting a single molecular pathway.

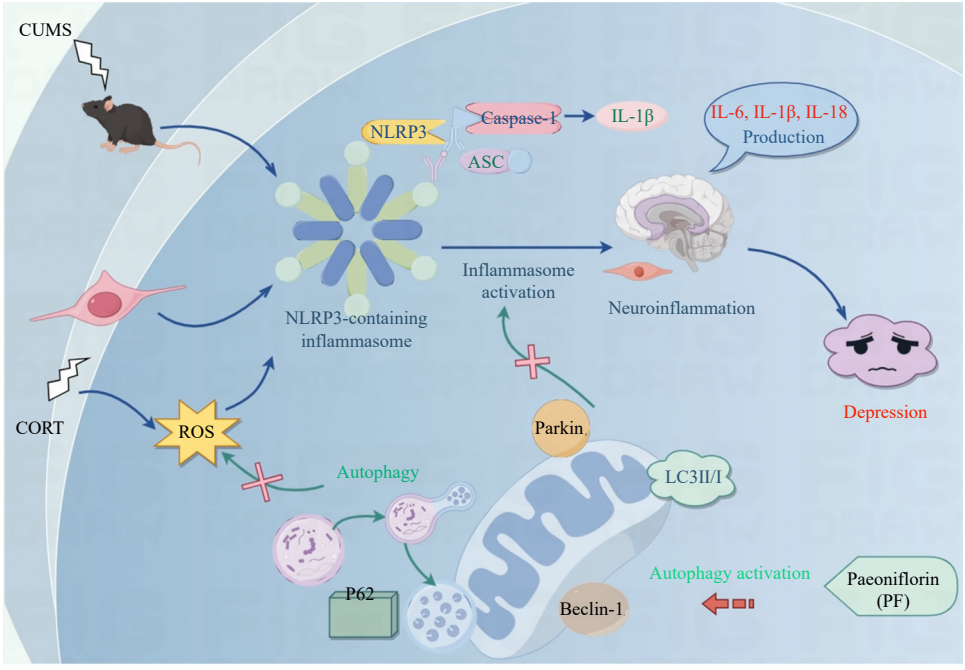

Fig. 9 PF alleviates depression by inhibiting the activation of NLRP3 inflammasome via promoting mitochondrial autophagy.

References

[1] Liu H, He YL, Wang JY, *et al*. Epidemiology of depression at Traditional Chinese Medicine Hospital in Shanghai, China [J]. *Compr Psychiatry*, 2016, **65**: 1-8.

[2] Rice F, Riglin L, Lomax T, *et al*. Adolescent and adult differences in major depression symptom profiles [J]. *J Affect Disord*, 2019, **243**: 175-181.

[3] Mukherjee N, Chaturvedi SK. Depressive symptoms and disorders in type 2 diabetes mellitus [J]. *Curr Opin Psychiatr*, 2019, **32**(5): 416-421.

[4] Maamri A, Ghabi H, Zalila H. Parkinson's disease and depression [J]. *Eur Psychiatr*, 2021, **64**: S240-S240.

[5] Pitman A, Suleman S, Hyde N, *et al*. Depression and anxiety in patients with cancer [J]. *BMJ*, 2018, **361**: k1415.

[6] Dwyer J B, Aftab A, Radhakrishnan R, *et al*. Hormonal treatments for major depressive disorder: state of the art [J]. *Am J Psychiatr*, 2020, **177**(8): 686-705.

[7] Chen L, Zhao X, Wei S, *et al*. Mechanism of paeoniflorin on ANIT-induced cholestatic liver injury using integrated metabolomics and network pharmacology [J]. *Front Pharmacol*, 2021, **12**: 737630.

[8] Li Y, Yin S, Chen X, *et al*. The inhibitory effect of paeoniflorin on reactive oxygen species alleviates the activation of NF-kappaB and MAPK signalling pathways in macrophages [J]. *Microbiology*, 2022, **168**(8): 001210.

[9] Niu K, Liu Y, Zhou Z, *et al*. Antitumor effects of paeoniflorin on Hippo signaling pathway in gastric cancer cells [J]. *J Oncol*, 2021, **2021**: 4724938.

[10] Han X, Hu S, Yang Q, *et al*. Paeoniflorin ameliorates airway inflammation and immune response in ovalbumin induced asthmatic mice: from oxidative stress to autophagy [J]. *Phytomedicine*, 2022, **96**: 153835.

[11] Guo K, Zhang Y, Li L, *et al*. Neuroprotective effect of paeoniflorin in the mouse model of Parkinson's disease through alpha-synuclein/protein kinase C delta subtype signaling pathway [J]. *Neuroreport*, 2021, **32**(17): 1379-1387.

[12] Zhang Y, Qiao L, Xu W, *et al*. Paeoniflorin attenuates cerebral ischemia-induced injury by regulating Ca(2 +)/CaMKII/CREB signaling pathway [J]. *Molecules*, 2017, **22**(3): 359.

[13] Qiu F, Zhong X, Mao Q, *et al*. The antidepressant-like effects of paeoniflorin in mouse models [J]. *Exp Ther Med*, 2013, **5**(4): 1113-1116.

[14] Li YC, Zheng XX, Xia SZ, *et al*. Paeoniflorin ameliorates depressive-like behavior in prenatally stressed offspring by restoring the HPA axis-and glucocorticoid receptor- associated dysfunction [J]. *J Affect Disord*, 2020, **274**: 471-481.

[15] Tang M, Chen M, Li Q. Paeoniflorin ameliorates chronic stress-induced depression-like behavior in mice model by affecting ERK1/2 pathway [J]. *Bioengineered*, 2021, **12**(2): 11329-11341.

[16] Cheng J, Chen M, Wan HQ, *et al*. Paeoniflorin exerts antidepressant-like effects through enhancing neuronal FGF-2 by microglial inactivation [J]. *J Ethnopharmacol*, 2021, **274**: 114046.

[17] Deretic V, Levine B. Autophagy balances inflammation in innate immunity [J]. *Autophagy*, 2018, **14**(2): 243-251.

[18] Ktistakis NT, Tooze SA. Digesting the expanding mechanisms of autophagy [J]. *Trends Cell Biol*, 2016, **26**(8): 624-635.

[19] Li C, Zhu Y, Wu Y, *et al*. Oridonin alleviates LPS-induced depression by inhibiting NLRP3 inflammasome *via* activation of autophagy [J]. *Front Med*, 2021, **8**: 813047.

[20] Swanson KV, Deng M, Ting JP. The NLRP3 inflammasome: molecular activation and regulation to therapeutics [J]. *Nat Rev Immunol*, 2019, **19**(8): 477-489.

[21] Ge C, Wang S, Wu X, *et al*. Quercetin mitigates depression-like behavior *via* the suppression of neuroinflammation and oxidative damage in corticosterone-induced mice [J]. *J Chem Neuroanat*, 2023, **2023**: 102313.

[22] Zhou Z, Wang Y, Sun S, *et al*. *Paeonia lactiflora* Pall. Polysaccharide alleviates depression in CUMS mice by inhibiting the NLRP3/ASC/Caspase-1 signaling pathway and affecting the composition of their intestinal flora [J]. *J Ethnopharmacol*, 2023, **316**: 116716.

[23] Ye JS, Chen L, Lu YY, *et al*. Honokiol-mediated mitophagy ameliorates postoperative cognitive impairment induced by surgery/sevoflurane *via* inhibiting the activation of NLRP3 inflammasome in the hippocampus [J]. *Oxid Med Cell Longev*, 2019, **2019**: 8639618.

[24] Chen K, Feng L, Hu W, *et al*. Optineurin inhibits NLRP3 inflammasome activation by enhancing mitophagy of renal tubular cells in diabetic nephropathy [J]. *FASEB J*, 2019, **33**(3): 4571-4585.

[25] Lyu D, Wang F, Zhang M, *et al*. Ketamine induces rapid antidepressant effects *via* the autophagy-NLRP3 inflammasome pathway [J]. *Psychopharmacology*, 2022, **239**(10): 3201-3212.

[26] Lu R, Zhang L, Yang X. Interaction between autophagy and the NLRP3 inflammasome in Alzheimer's and Parkinson's disease [J]. *Front Aging Neurosci*, 2022, **14**: 1018848.

[27] Shu X, Sun Y, Sun X, *et al*. The effect of fluoxetine on astrocyte autophagy flux and injured mitochondria clearance in a mouse model of depression [J]. *Cell Death Dis*, 2019, **10**(8): 577.

[28] Sun X, Zhang T, Zhao Y, *et al*. Panaxynol attenuates CUMS-induced anxiety and depressive-like behaviors *via* regulating neurotransmitters, synapses and the HPA axis in mice [J]. *Food Funct*, 2020, **11**(2): 1235-1244.

[29] Willner P, Towell A, Sampson D, *et al*. Reduction of sucrose preference by chronic unpredictable mild stress, and its restoration by a tricyclic antidepressant [J]. *Psychopharmacology (Berl)*, 1987, **93**(3): 358-64.

[30] Carola V, D'Olimpio F, Brunamonti E, *et al*. Evaluation of the elevated plus-maze and open-field tests for the assessment of anxiety-related behaviour in inbred mice [J]. *Behav Brain Res*, 2002, **134**(1-2): 49-57.

[31] Perez-Caballero L, Torres-Sanchez S, Bravo L, *et al*. Fluoxetine: a case history of its discovery and preclinical development [J]. *Expert Opin Drug Discov*, 2014, **9**(5): 567-578.

[32] Duman RS, Monteggia LM. A neurotrophic model for stress-related mood disorders [J]. *Biol Psychiatry*, 2006, **59**(12): 1116-1127.

[33] Nutt DJ. Relationship of neurotransmitters to the symptoms of major depressive disorder [J]. *Clin Psychiatry*, 2008, **69 Suppl E1**: 4-7.

[34] Brakel K, Hook MA. SCI and depression: does inflammation commandeer the brain? [J]. *Exp Neurol*, 2019, **320**: 112977.

[35] Yang Y, Wang H, Kouadir M, *et al*. Recent advances in the mechanisms of NLRP3 inflammasome activation and its inhibitors [J]. *Cell Death Dis*, 2019, **10**(2): 128.

[36] Troubat R, Barone P, Leman S, *et al*. Neuroinflammation and depression: a review [J]. *Eur J Neurosci*, 2021, **53**(1): 151-171.

[37] Nguyen C, Boutron I, Baron G, *et al*. Intradiscal glucocorticoid injection for patients with chronic low back pain associated with active discopathy: a randomized trial [J]. *Ann Intern Med*, 2017, **166**(8): 547-556.

[38] Zhao X, Cao F, Liu Q, *et al*. Behavioral, inflammatory and neurochemical disturbances in LPS and UCMS-induced mouse models of depression [J]. *Behav Brain Res*, 2019, **364**: 494-502.

[39] Liu H, You L, Wu J, *et al*. Berberine suppresses influenza virus-triggered NLRP3 inflammasome activation in macrophages by inducing mitophagy and decreasing mitochondrial ROS [J]. *J Leukoc Biol*, 2020, **108**(1): 253-266.

Cite this article as: SU Lili, GUO Pengli, GUO Xiangjuan, *et al*. Paeoniflorin alleviates depression by inhibiting the activation of NLRP3 inflammasome *via* promoting mitochondrial autophagy [J]. *Chin J Nat Med*, 2024, **22**(6): 515-529.